

Toward Active Current Density Profile Control in NSTX-U: *Performance Assessment via Predictive TRANSP Simulations*

Zeki Ilhan¹, William P. Wehner¹, Eugenio Schuster¹,
Mark D. Boyer², David A. Gates², Stefan P. Gerhardt², Jonathan E. Menard²

¹Department of Mechanical Engineering & Mechanics
Lehigh University

²Princeton Plasma Physics Laboratory

zeki.ilhan@lehigh.edu

18th International Spherical Torus Workshop

November 4, 2015



Motivation for Current Density Profile Control in NSTX-U

- There is growing consensus that the path to an economical power-producing reactor is the “Advanced Tokamak” (AT) concept.
- AT operational goals for the NSTX-U include [1]:
 - Non-inductive sustainment of the high- β spherical torus. (Fusion power scales as $P_{fus} \approx \beta^2 B^4$)
 - High performance equilibrium scenarios with neutral beam heating.
 - Longer pulse durations.
- Active, model-based, feedback control of the current density profile evolution can be useful to achieve these AT operational goals.
- Relation between ι -profile and the toroidal current density (j_ϕ) profile [2]:

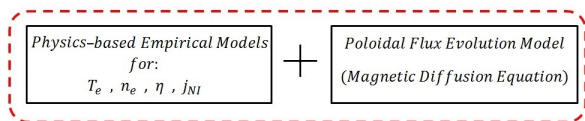
$$\iota(\hat{\rho}, t) = \frac{R_0 \mu_0}{\hat{\rho}^2 B_\phi} \int_0^{\hat{\rho}} j_\phi(\hat{\rho}', t) \hat{\rho}' d\hat{\rho}' = \underbrace{-\frac{d\Psi}{d\Phi}}_{-(\partial\psi/\partial\hat{\rho})/B_{\phi,0}\rho_b^2\hat{\rho}}$$

- Control of the ι -profile is equivalent to control of the current density profile, $j_\phi(\hat{\rho}, t)$, and the control of the poloidal flux gradient profile, $\partial\psi/\partial\hat{\rho}$.

[1] GERHARDT, S. P., ANDRE, R., and MENARD, J. E., Nuclear Fusion **52** (2012).

[2] J. Wesson, *Tokamaks* (Oxford University Press, 3rd edition, 2004).

First-Principles-Driven (FPD) Current Profile Modeling



First – Principles – Driven (FPD) Current Profile Evolution Model

- The evolution of the **poloidal magnetic flux** is given by the **Magnetic Diffusion Equation [3]**

$$\frac{\partial \psi}{\partial t} = \frac{\eta(T_e)}{\mu_0 \rho_b^2 \hat{F}^2} \frac{1}{\hat{\rho}} \frac{\partial}{\partial \hat{\rho}} \left(\hat{\rho} D_\psi \frac{\partial \psi}{\partial \hat{\rho}} \right) + R_0 \hat{H} \eta(T_e) \frac{\langle \bar{j}_{NI} \cdot \bar{B} \rangle}{B_{\phi,0}}, \quad (1)$$

with boundary conditions

$$\left. \frac{\partial \psi}{\partial \hat{\rho}} \right|_{\hat{\rho}=0} = 0, \quad \left. \frac{\partial \psi}{\partial \hat{\rho}} \right|_{\hat{\rho}=1} = -\frac{\mu_0}{2\pi} \frac{R_0}{\hat{G} \Big|_{\hat{\rho}=1} \hat{H} \Big|_{\hat{\rho}=1}} I(t), \quad (2)$$

where $D_\psi(\hat{\rho}) = \hat{F}(\hat{\rho}) \hat{G}(\hat{\rho}) \hat{H}(\hat{\rho})$, and \hat{F} , \hat{G} , \hat{H} are geometric factors pertaining to the magnetic configuration of a particular equilibrium.

[3] OU, Y., LUCE, T. C., SCHUSTER E. et al., *Fusion Engineering and Design* (2007).

First-Principles-Driven (FPD) Current Profile Modeling

- NSTX-U-tailored [4] empirical models [5] for the electron temperature, electron density, plasma resistivity, and noninductive current drives [6] take the form

$$n_e(\hat{\rho}, t) = n_e^{prof}(\hat{\rho})u_n(t) \quad (3)$$

$$T_e(\hat{\rho}, t) = k_{T_e}(\hat{\rho}, t_r) \frac{T_e^{prof}(\hat{\rho}, t_r)}{n_e(\hat{\rho}, t)} I(t) \sqrt{P_{tot}(t)} \quad (4)$$

$$\eta(T_e) = \frac{k_{sp}(\hat{\rho}, t_r) Z_{eff}}{T_e(\hat{\rho}, t)^{3/2}} \quad (5)$$

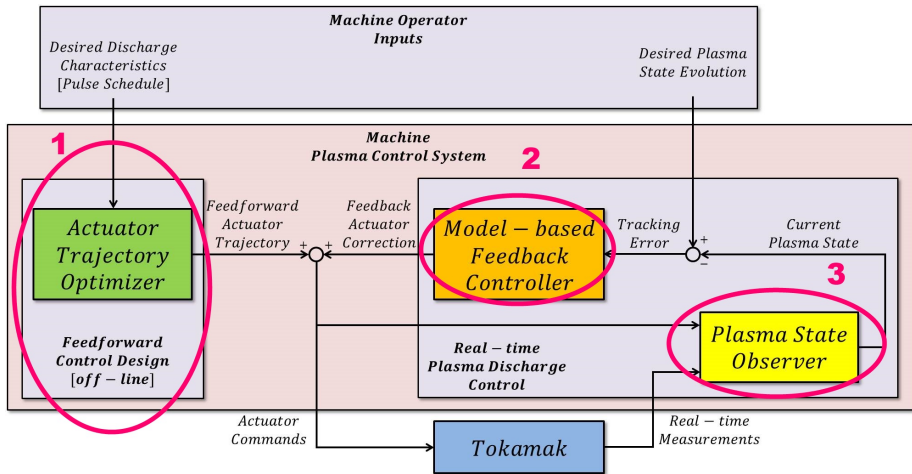
$$\begin{aligned} \frac{\langle \bar{\mathbf{j}}_{ni} \cdot \bar{\mathbf{B}} \rangle}{B_{\phi,0}} &= \sum_{i=1}^6 \frac{\langle \bar{\mathbf{j}}_{nbi_i} \cdot \bar{\mathbf{B}} \rangle}{B_{\phi,0}} + \frac{\langle \bar{\mathbf{j}}_{bs} \cdot \bar{\mathbf{B}} \rangle}{B_{\phi,0}} \\ &= \sum_{i=1}^6 k_i^{prof}(\hat{\rho}) J_i^{dep}(\hat{\rho}) \frac{\sqrt{T_e(\hat{\rho}, t)}}{n_e(\hat{\rho}, t)} P_i(t) \\ &\quad + \frac{k_{JeV} R_0}{\hat{F}(\hat{\rho})} \left(\frac{\partial \psi}{\partial \hat{\rho}} \right)^{-1} \left[2\mathcal{L}_{31} T_e \frac{\partial n_e}{\partial \hat{\rho}} + \{2\mathcal{L}_{31} + \mathcal{L}_{32} + \alpha \mathcal{L}_{34}\} n_e \frac{\partial T_e}{\partial \hat{\rho}} \right] \end{aligned} \quad (6)$$

[4] ILHAN, Z. O. et al., 55th Annual Meeting of the APS DPP (2013)

[5] BARTON, J. E. et al., 52nd IEEE CDC (2013)

[6] SAUTER, O. et al., Physics of Plasmas (1999), (2002)

Possible Uses of the FPD Model



Schematics of the plasma profile control system

Feedforward Actuator Trajectory Optimization

- **Objective:** Design the actuator trajectories that can steer the plasma to a target state characterized by the safety factor profile $q^{tar}(\hat{\rho}, t_f)$ or rotational transform profile $\iota^{tar}(\hat{\rho}, t_f)$ at a specified time t_f during the discharge such that the achieved plasma state is as stationary in time as possible.
- **Cost functional** defined as:

$$J(t_f) = k_q J_q(t_f) + k_{ss} J_{ss}(t_f)$$

where k_{ss} and k_q are the weight factors representing the relative importance of the plasma state characteristics and

$$J_q(t_f) = \int_0^1 W_q(\hat{\rho}) [q^{tar}(\hat{\rho}) - q(\hat{\rho}, t_f)]^2 d\hat{\rho} \quad (7)$$

$$J_{ss}(t_f) = \int_0^1 W_{ss}(\hat{\rho}) [g_{ss}(\hat{\rho}, t_f)]^2 d\hat{\rho}, \quad (8)$$

where $W_q(\hat{\rho})$ and $W_{ss}(\hat{\rho})$ are positive weight functions and

$$g_{ss}(\hat{\rho}, t) = \frac{\partial U_p}{\partial \hat{\rho}} = -\frac{\partial \Psi}{\partial t} = -2\pi \frac{\partial \psi}{\partial t}, \quad (9)$$

where U_p is the loop-voltage profile which can be related to the temporal derivative of the poloidal magnetic flux.

Formulation of Various Constraints

- **Actuator Trajectory Parametrization:** The trajectories of the i -th control actuator (u_i) can be parametrized by a finite number n_{p_i} of *to-be-determined parameters* (x_i) at discrete points in time (t_{p_i}), i.e.,

$$t_{p_i} = [t_1, t_2, \dots, t_k, \dots, t_{n_{p_i}} = t_f] \in \mathbb{R}^{n_{p_i}}$$

$$x_i = [u_i^1, u_i^2, \dots, u_i^k, \dots, u_i^{n_{p_i}}] \in \mathbb{R}^{n_{p_i}}$$

- Combining all parameters to represent individual actuator trajectories into the vector \tilde{x} , where $\tilde{x} \in \mathbb{R}^{n_p^{tot}}$ and $n_p^{tot} = \sum_{i=1}^{n_{act}} n_{p_i}$, the control actuator trajectories can be written compactly as

$$\boxed{u(t) = \Pi(t)\tilde{x}} \quad (10)$$

- **Actuator Constraints:** The actuator magnitude and rate constraints are given by

$$I_p^{min} \leq I_p(t) \leq I_p^{max},$$

$$P_i^{min} \leq P_i(t) \leq P_i^{max}, \quad i = 1, \dots, n_{nbi}$$

$$-I_{p,max}^{d'} \leq dI_p/dt \leq I_{p,max}^{u'}$$

- The above actuator constraints can be written compactly as a matrix inequality as

$$\boxed{A_u^{lim} \tilde{x} \leq b_u^{lim}} \quad (11)$$

Statement of the Optimization Problem

- The optimization problem is written mathematically as

$$\min_{\tilde{x}} J(t_f) = J(\dot{\theta}(t_f), \theta(t_f)), \quad (12)$$

such that

$$\dot{\theta} = g(\theta, u), \quad (13)$$

$$u(t) = \Pi(t)\tilde{x}, \quad (14)$$

$$A_u^{lim}\tilde{x} \leq b_u^{lim}, \quad (15)$$

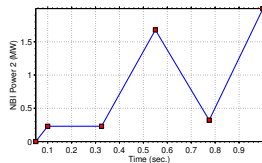
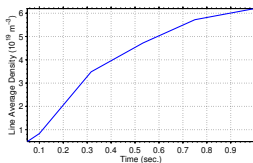
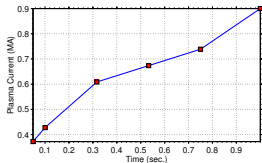
where the **poloidal flux gradient**, $\theta = d\psi/d\hat{\rho}$ represents the plasma state, u represents the actuators, and g is a nonlinear function representing the plasma dynamics as an additional constraint ((13) is derived from (1)-(6)).

- The optimization problem (12)-(15) can be solved iteratively in MATLAB by using the **Sequential Quadratic Programming (SQP)** method [7].

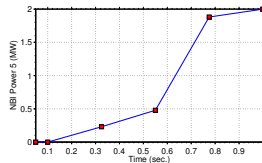
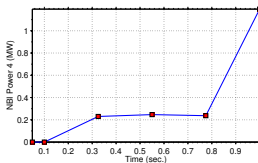
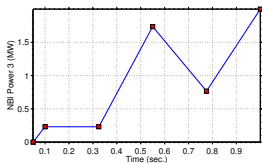
[7] J. Nocedal and S. J. Wright, *Numerical optimization*, (Springer, New York, 2006).

Feedforward Optimization: Weighting only the q -profile

- For this application, $k_q = 1$ and $k_{ss} = 0$ in the cost functional.
- **The goal is to hit a target q -profile at $t_f = 1$ sec.**



(a) Optimal plasma current $I_p(t)$ (b) Line Averaged Density $\bar{n}_e(t)$ (c) Optimal NBI beam power #2

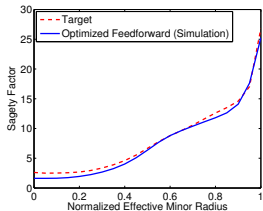


(d) Optimal NBI beam power #3 (e) Optimal NBI beam power #4 (f) Optimal NBI beam power #5

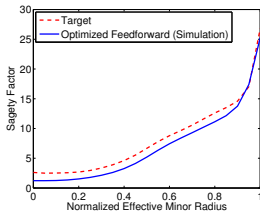
Time evolution of the optimized feedforward actuator trajectories

Feedforward Optimization: Weighting only the q -profile

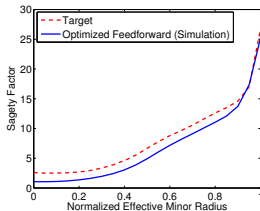
- Comparison of the target and achieved q -profiles at various times:



(a) $t = t_f = 1.0$ sec.

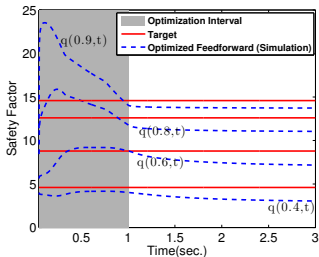


(b) $t = 2.0$ sec.



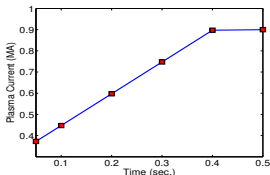
(c) $t = 3.0$ sec.

- Time evolution of the safety factor at various radial locations:

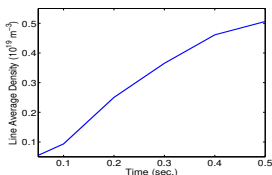


Feedforward Optimization: Weighting only Steadiness

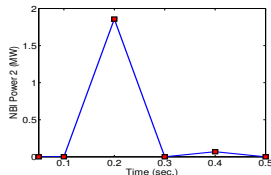
- For this application, $k_{ss} = 1$ and $k_q = 0$ in the cost functional.
- **The goal is to maintain a steady q -profile throughout the simulation.**



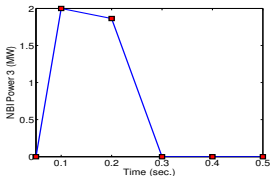
(a) Optimal plasma current $I_p(t)$



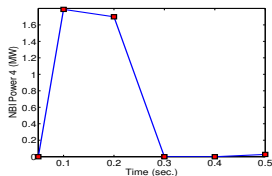
(b) Line Averaged Density



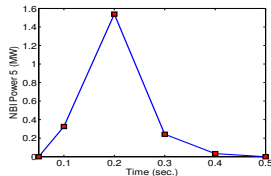
(c) Optimal NBI beam power #2



(d) Optimal NBI beam power #3



(e) Optimal NBI beam power #4

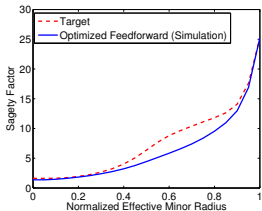


(f) Optimal NBI beam power #5

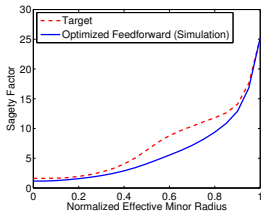
Time evolution of the optimized feedforward actuator trajectories

Feedforward Optimization: Weighting only Steadiness

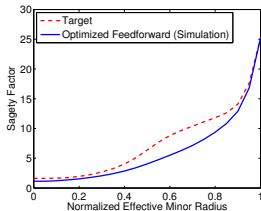
- Comparison of the target and achieved q -profiles at various times:



(a) $t = t_f = 0.5$ sec.

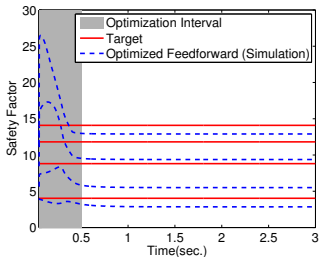


(b) $t = 1.0$ sec.



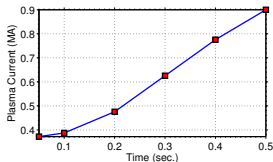
(c) $t = 2.0$ sec.

- Time evolution of the safety factor at various radial locations:

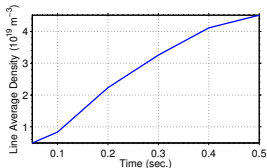


Feedforward Optimization: Weighting q + Steadiness

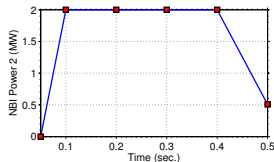
- For this application, $k_{ss} = 1$ and $k_q = 1$ in the cost functional.
- **The goal is to hit a target q -profile at $t = 0.5$ sec. and maintain it throughout a 3 sec. simulation.**



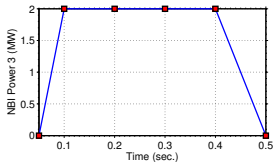
(a) Optimal plasma current $I_p(t)$



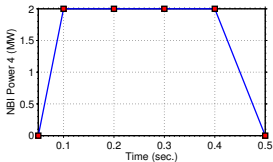
(b) Line Averaged Density



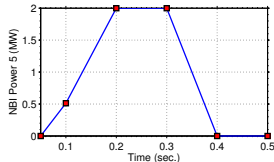
(c) Optimal NBI beam power #2



(d) Optimal NBI beam power #3



(e) Optimal NBI beam power #4

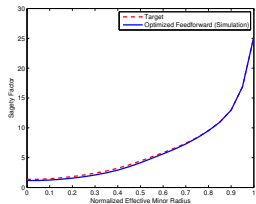


(f) Optimal NBI beam power #5

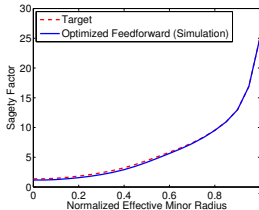
Time evolution of the optimized feedforward actuator trajectories

Feedforward Optimization: Weighting q + Steadiness

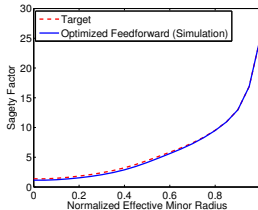
- Comparison of the target and achieved q -profiles at various times:



(a) $t = t_f = 0.5$ sec.

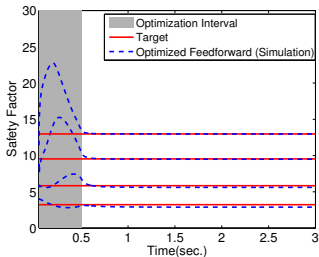


(b) $t = 1.0$ sec.



(c) $t = 2.0$ sec.

- Time evolution of the safety factor at various radial locations:



Optimal Feedback Control of the Current Density Profile

- **Linear-Quadratic-Integral (LQI)** Optimal feedback controller has been designed in **MATLAB** based on the **FPD, control-oriented model**.
- The **effectiveness** of the designed **controller** is **first tested in MATLAB** by simulating the nonlinear **magnetic diffusion equation (1)**.
- Early results on control design and numerical testing have been presented in **[8], [9]**.
- The **proposed feedback controller is now implemented in TRANSP** for performance assessment before experimental testing in NSTX-U.
- Recently developed **Expert routine [10]** provides a **framework** to perform **closed-loop predictive simulations** within the **TRANSP source code**.

[8] ILHAN, Z. O. et al., 56th Annual Meeting of the APS DPP (2014)

[9] ILHAN, Z. O. et al., IEEE Multi-Conference on Systems and Control (2015)

[10] BOYER, M. D., ANDRE, R., GATES, D. A., et al., Nuclear Fusion **55 (2015)**

Closed-Loop Control Simulation Study in TRANSP

- The control objective is to track a target state trajectory $u_r(\rho, t)$ with *minimum control effort*.
- The target state trajectory $u_r(\rho, t)$ is generated through an open-loop TRANSP simulation with the following constant reference inputs.

$n_e(\text{m}^{-3})$	5.0×10^{19}	$P_4(\text{W})$	0.8×10^6
$P_1(\text{W})$	0.2×10^6	$P_5(\text{W})$	1.0×10^6
$P_2(\text{W})$	0.4×10^6	$P_6(\text{W})$	1.2×10^6
$P_3(\text{W})$	0.6×10^6	$I_p(\text{A})$	0.7×10^6

- Starting from the first second of the simulation, the controller is tested against *perturbed initial conditions* and *constant input disturbances*, i.e.,

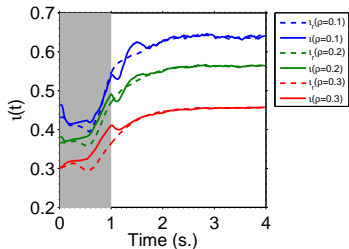
$$u(t) = \begin{cases} u_r + u_d, & t \leq 1 \text{ s.} \\ u_r + u_d + \Delta u(t), & t > 1 \text{ s.} \end{cases}$$

where u_r represents the constant reference inputs, u_d stands for the constant disturbance inputs (15% for I_p , 10% for P_1 , P_3 , P_5 and P_6), and $\Delta u(t)$ is the output of the feedback controller.

CASE 1: Actuation with I_p and Neutral Beams

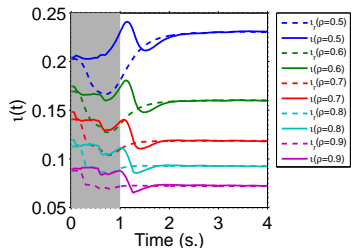
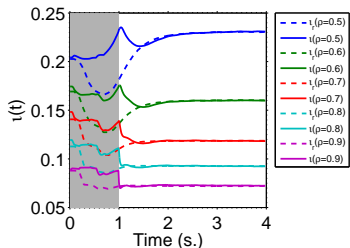
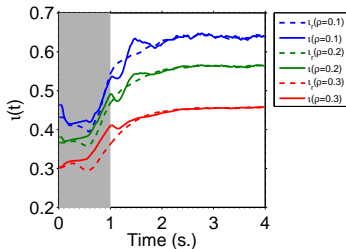
CASE 1A

(without I_p rate saturation)



CASE 1B

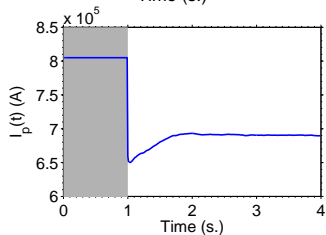
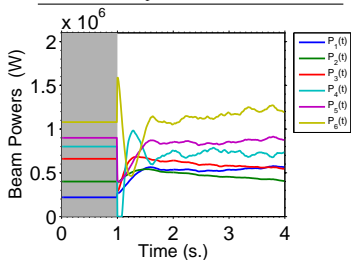
(with I_p rate saturation)



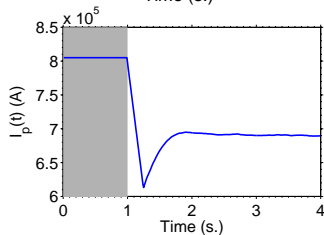
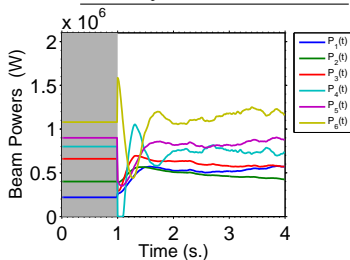
Figures (left & right): Time evolution of the optimal outputs (solid) with their respective targets (dashed). Controller is off in the grey region.

CASE 1: Actuation with I_p and Neutral Beams

CASE 1A
(without I_p rate saturation)



CASE 1B
(with I_p rate saturation)

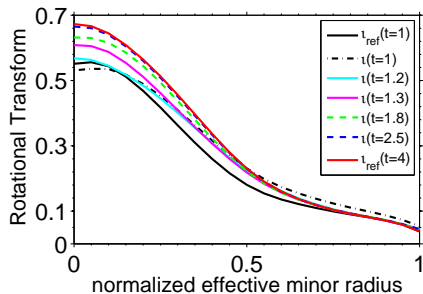


Figures (upper left & right): Time evolution of the optimal beam powers.
Figures (lower left & right): Time evolution of the optimal plasma current.

CASE 1: Actuation with I_p and Neutral Beams

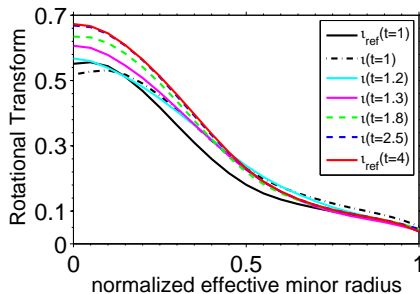
CASE 1A

(without I_p rate saturation)



CASE 1B

(with I_p rate saturation)

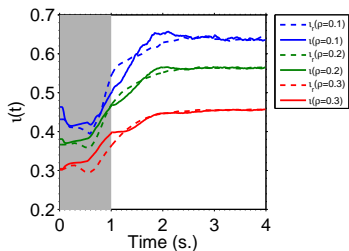


Figures (left & right): Time evolution of the rotational transform (l -profile).

CASE 2: Actuation with n_e , I_p and Neutral Beams

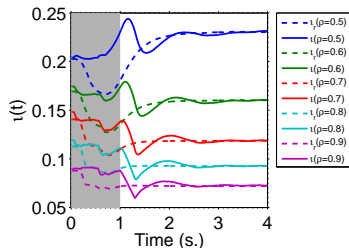
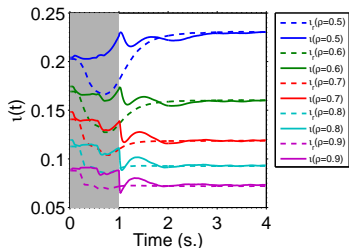
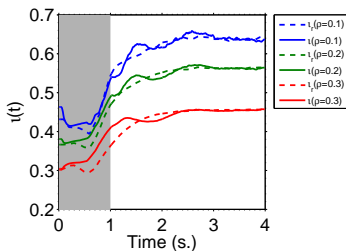
CASE 2A

(without I_p & n_e rate saturation)



CASE 2B

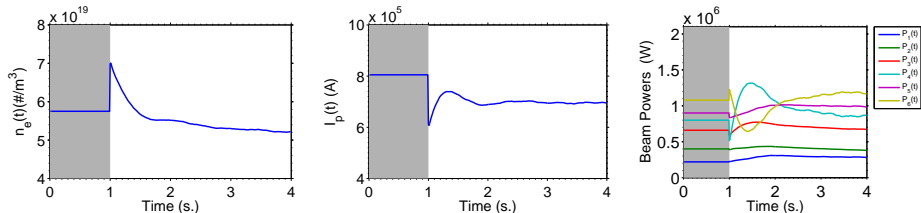
(with I_p & n_e rate saturation)



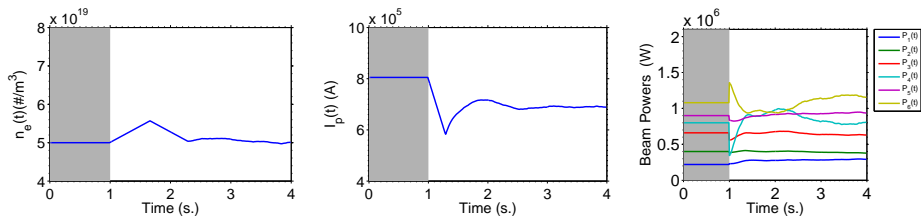
Figures (left & right): Time evolution of the optimal outputs (solid) with their respective targets (dashed). Controller is off in the grey region.

CASE 2: Actuation with n_e , I_p and Neutral Beams

● CASE 2A (without I_p & n_e rate saturation)



● CASE 2B (with I_p & n_e rate saturation)

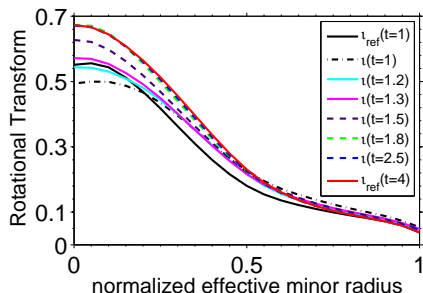


Figures: (left) Time evolution of the optimal line-averaged electron density, (center) time evolution of the optimal plasma current, and (right) time evolution of the optimal beam powers.

CASE 2: Actuation with n_e , I_p and Neutral Beams

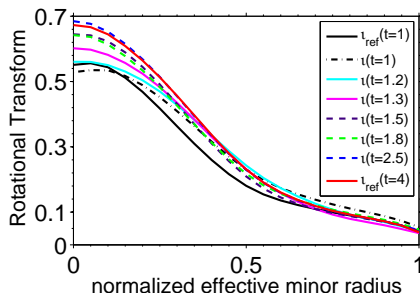
CASE 2A

(without I_p & n_e rate saturation)



CASE 2B

(with I_p & n_e rate saturation)



Figures (left & right): Time evolution of the rotational transform (l -profile).

CASE 3: Control Against Changing Confinement Factor

- In predictive TRANSP simulations, n_e and T_e profile evolutions are *not modeled by first-principles calculations*. [11]
- A reference n_e profile is specified based on an experimental profile measured on NSTX and then scaled to achieve a particular Greenwald fraction, f_{GW} .
- Similarly, T_e profile is also taken from an experiment and scaled to achieve a particular global confinement time [12]

$$\tau_{ST} = H_{ST} 0.1178 I_p^{0.57} B_T^{1.08} n_e^{0.44} P_{Loss,th}^{-0.73}$$

- When performing closed-loop simulations in TRANSP, the simulation **must be constrained to follow a specific confinement level all the time** although the actuators are varied based on the calculations of the feedback controller \Rightarrow This is achieved by **manipulating** the confinement factor H_{ST} through a **user-defined waveform**. [13]
- However, the H_{ST} factor **can deviate** from the user-supplied waveform in the NSTX-U experiments \Rightarrow **creating additional source of disturbance**.

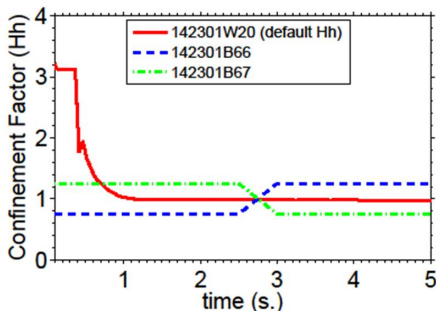
[11] GERHARDT, S. P., ANDRE, R., and MENARD, J. E., Nuclear Fusion **52** (2012).

[12] KAYE, S. et al., Nuclear Fusion **46** (2006).

[13] BOYER, M. D., ANDRE, R., GATES, D. A., et al., Nuclear Fusion **55** (2015).

CASE 3: Control Against Changing Confinement Factor

- Two closed-loop TRANSP simulations are carried out to verify disturbance rejection against changing confinement factors:
 - Run 142301B66 has a step increase in the H_{ST} from 0.75 to 1.25.
 - Run 142301B67 has a step decrease in the H_{ST} from 1.25 to 0.75.
- Note that the target profile corresponds to the open-loop run 142301W20, which has $H_{ST} \approx 1$ when $t \in [1, 5]$ s., during which the controller is on.
- Only I_p and neutral beams are used as actuators without considering rate saturations.

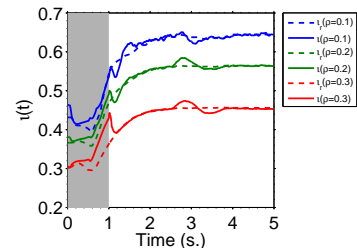


Time evolution of the confinement factors.

CASE 3: Control Against Changing Confinement Factor

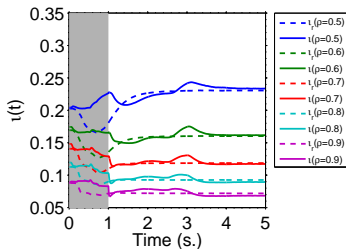
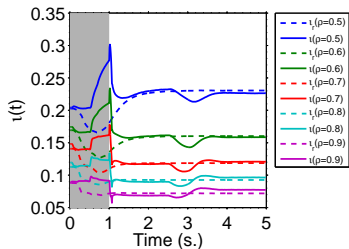
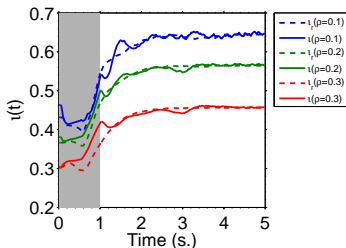
CASE 3A

(increasing H_{ST} - 142301B66)



CASE 3B

(decreasing H_{ST} - 142301B67)

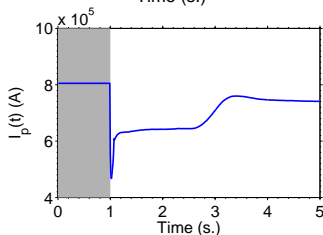
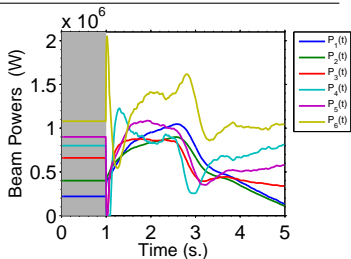


Figures (left & right): Time evolution of the optimal outputs (solid) with their respective targets (dashed). Controller is off in the grey region.

CASE 3: Control Against Changing Confinement Factor

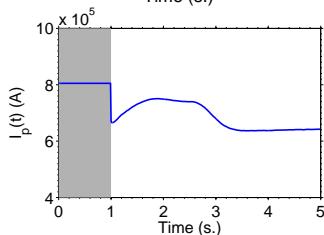
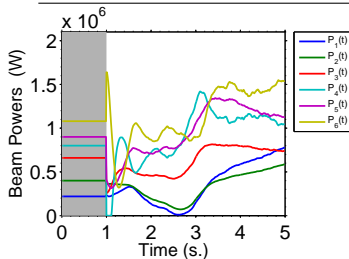
CASE 3A

(increasing H_{ST} - 142301B66)



CASE 3B

(decreasing H_{ST} - 142301B67)

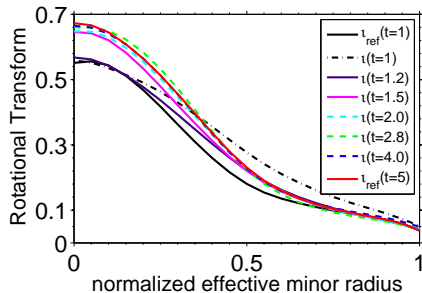


Figures (upper left & right): Time evolution of the optimal beam powers.
Figures (lower left & right): Time evolution of the optimal plasma current.

CASE 3: Control Against Changing Confinement Factor

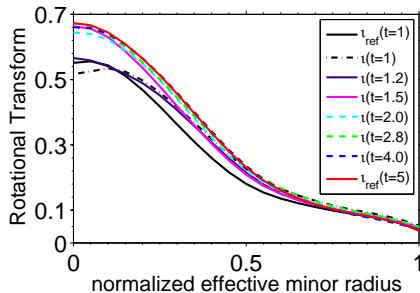
CASE 3A

(increasing H_{ST} - 142301B66)



CASE 3B

(decreasing H_{ST} - 142301B67)



Figures (left & right): Time evolution of the rotational transform (l -profile).

Conclusion and Future Work

- A nonlinear, control-oriented, physics-based model has been proposed to describe the evolution of the poloidal magnetic flux profile, which can be related to the q -profile (ι -profile) \Rightarrow the current density profile.
- Using this first-principles-driven (FPD), control-oriented model, a **two-component control design** approach has been proposed for the regulation of the current density profile:
 - 1 **A feedforward trajectory optimizer** (controller) to compute offline actuator requests to achieve specific plasma scenarios.
 - 2 **A feedback control algorithm** to track a desired current density profile while adding robustness against model uncertainties and disturbances to the overall current profile control scheme.
- **The performance of the feedback controller has been validated in TRANSP simulations through the recently developed Expert routine**, which provides a framework to perform closed-loop predictive simulations within the TRANSP source code.
- **The immediate next step** is to test the feedforward actuator trajectory optimizer in TRANSP and then in the actual NSTX-U machine.
- **A longer-term next step** is the implementation of the feedback controller in the NSTX-U PCS with the ultimate goal of experimental testing.